Optical and Quantum Electronics **36:** 259–269, 2004.

Ring microresonator as a photonic structure with complex eigenfrequency

LADISLAV PRKNA, JIŘÍ ČTYROKÝ* AND MILAN HUBÁLEK
Institute of Radio Engineering and Electronics ASCR, Chaberská 57, 182 51 Praha 8, Czech Republic
*(*author for correspondence: E-mail: ctyroky@ure.cas.cz)*

Abstract. For the analysis of light propagation in photonic guided-wave ring microresonators, leaky-mode solvers for bent channel waveguides are often used. In the analytical approach, the leaky mode field is expressed in terms of cylindrical functions of complex arguments and a complex order which plays a role of the (azimuthal) propagation constant. In this contribution we present a modified approach which takes into account the circular symmetry of the structure. We calculate the eigenmodes of a lossy microresonator as modes with complex eigenfrequencies. In this approach, the eigenmodes are described by cylindrical functions of an integer order and a complex argument. Similarities and differences of both approaches are demonstrated using simple examples of 2D (planar) structures.

Key words: complex frequency, microresonators, optical waveguide theory

1. Introduction

Photonic guided-wave devices based on ring microresonators are very promising guided-wave structures with many potential applications in optical communication systems. They can be used for various functions like spectral filtering, space switching, modulation, add/drop multiplexing etc. At the same time they offer considerable technological uniformity and potential for large-scale integration and batch processing that could lead to inexpensive fabrication of photonic devices. Important applications of microresonator-based components especially in photonic access and metropolitan area networks are thus envisaged.

Theory, design, fabrication and applications of microresonators based on circular ring channel waveguides with lateral or vertical coupling to a signal input/output bus have been subject of intense recent research, see, e.g., (Little *et al.* 1977; Chin *et al.* 1998; Chu *et al.* 1999; Little *et al.* 2000; Yariv 2000; Klunder *et al.* 2002). To get an insight to the wave processes in the ring microresonator coupled to the straight input/output channel waveguide, the finite-difference time domain (FDTD) method is frequently used (Little *et al.* 1988). However, for modelling real structures, the number of grid points needs to be high, which makes the calculations rather demanding on memory and time.

Modal methods can be considered complementary in such a sense that they posses good physical insight with moderate computational power but become rather complex for more complex geometries. The circular ring microresonator is a structure with 2D refractive-index distribution (independent of the azimuthal co-ordinate), so that mode matching method can be applied to advantage (Manolatou *et al.* 1999). The basic task is apparently to find eigenmodes of the microresonator. The coupling to the straight bus guide can then be calculated with a reasonable degree of accuracy using the coupled-mode theory (Loaiza *et al.* 2000).

Light propagation in ring microresonators is often modelled with mode solvers for bent channel waveguides. In the circularly bent waveguide with the refractive index distribution independent of the azimuthal co-ordinate φ, the field distribution is separable into the form

$$\mathbf{E}(r, \varphi, z) = \mathbf{F}(r, z) \exp(\pm \mathrm{i} v \varphi). \tag{1}$$

Here, (r, φ, z) is a cylindrical co-ordinate system, $\mathbf{E}$ is electric field intensity vector of the optical wave, and $\mathbf{F}$ is a suitable vectorial function. The classical concept of the effective refractive index of the waveguide mode looses for the bent waveguide its proper physical sense – it is namely no more the eigenvalue of the problem. Its role was taken over by the azimuthal index v, as follows from (1). The effective refractive index can be formally defined as follows:

$$n_{\mathrm{eff}} = v/(k_0 R), \tag{2}$$

where R is a suitably defined radius of curvature of the waveguide, $k_0 = 2\pi/\lambda$ is the wavenumber, λ is the free space wavelength. The radius of curvature of the waveguide can be defined rather deliberately (i.e., from the centre of curvature to the inner or outer edge of the guide or to its centre), and each choice leads to different value of n_{eff}.

Due to radiation from the bent waveguide, the eigenmodes are inevitably leaky. This leaky character of the waveguide is manifested by the fact that the azimuthal index v becomes complex, $v = v' + \mathrm{i}v''$. Supposing the (suppressed) harmonic time dependence of the form $\exp(-\mathrm{i}\omega t)$, the imaginary parts of v and thus also n_{eff} in a leaky waveguide are positive.

At resonance, the phase change per roundtrip

$$\Delta\phi = 2\pi v' = 2\pi k_0 n'_{\mathrm{eff}} R, \tag{3}$$

must be equal to an integer multiple of 2π. The resonance wavelength can be found from the condition $v'(\lambda) = m$, where m is a suitable integer. The quality factor of the resonator Q_v and its finesse F_v at the resonant wavelength is then

usually expressed in terms of the complex azimuthal index or the complex effective index as

$$Q_v = \frac{v'}{2v''} = \frac{n'_{\text{eff}}}{2n''_{\text{eff}}}, \qquad F_v = \frac{Q_v}{v'} = \frac{1}{2v''}. \tag{4}$$

In this contribution we present a slightly different approach which takes into account the circular symmetry of the resonator as a whole. The eigenmodes of a microresonator are considered as modes of a rotationally symmetric structure with the azimuthal dependence $\exp(\mathrm{i}v\varphi)$. Because of rotational symmetry, this function must be periodical with a period of 2π, and thus v must be an integer. Lossy character of the resonator is then manifested by nonzero imaginary parts of its eigenfrequency ω_0 (or equivalently, by the complex wavenumbers $k_0 = \omega_0/c$, c being the velocity of light *in vacuo*). The complex frequency is a simple way how to describe the decaying time-harmonic process, $\exp(-\mathrm{i}\omega t) = \exp(-\mathrm{i}\omega' t)\exp(-|\omega''|t)$, that takes place in a lossy resonator without feeding.

The concept of the complex frequency of a lossy resonator is analogical to the commonly used concept of the complex propagation constant of a lossy guide. Both the propagation constant of a guide and the resonant frequency of a resonator are eigenvalues of pertinent wave equations which become complex in the presence of loss (or gain). The complex frequency approach to resonant systems is by far not new – it can be traced back to the late thirties of the 20th century when the complex frequency was used to describe the resonant frequency and the Q-factor of a metallic microwave cavity. Since then, it has been frequently applied in physics and engineering to describe eigenfrequencies of various systems with loss or gain.

For better insight into the interdependencies of both approaches, let us first consider a very simple electrical serial resonant RLC circuit. Using the time dependence $\exp(-\mathrm{i}\omega t)$, its resonant condition can be written as

$$-\mathrm{i}\omega L - 1/\mathrm{i}\omega C + R = 0.$$

The resonant frequency in the absence of loss ($R = 0$) is $\omega_0 = 1/\sqrt{LC}$. Supposing that the quality factor of the circuit $Q = \omega_0 L/R$ is large compared to unity, the solution of the resonant condition can be expressed in the form

$$\omega \approx \omega_0\left(1 - \frac{\mathrm{i}}{2Q}\right), \tag{5}$$

where terms of the order of $1/Q^2$ and higher were neglected.

As the next step, let us consider the ring resonator as a circular loop of a radius R made of a lossy guide with the complex propagation constant $\beta = k_0 n_{\text{eff}} = k_0(n'_{\text{eff}} + \mathrm{i}n''_{\text{eff}})$. The resonant condition for the resonator can be

written in the form $k_0 n_{\text{eff}} R = v$, where v is a (real) integer. If n_{eff} is complex, k_0 must be complex as well, to fulfill the resonant condition $(k_0' + \mathrm{i}k_0'')$ $(n_{\text{eff}}' + in_{\text{eff}}'') = v/R$. Supposing that the spectral dependence of the effective index in the narrow bandwidth of a high-quality resonator is unimportant, we find

$$k_0' \approx v/Rn_{\text{eff}}', \qquad Q_v \approx -\frac{k_0'}{2k_0''} = \frac{n_{\text{eff}}'}{2n_{\text{eff}}''}, \qquad F_v = \frac{Q_v}{v} \approx -\frac{k_0'}{2vk_0''} = \frac{n_{\text{eff}}'}{2vn_{\text{eff}}''}. \quad (6)$$

Comparing this with Equations (3) and (4), it is apparent that both approaches give essentially identical results.

In the following we apply both approaches to simple 2D ('planar') ring and disk microresonator structures. Modelling more complex 3D resonator structures can follow the same guidelines, as it is briefly discussed in the last section.

Note that the complex frequency approach described here is useful not only for searching eigenmodes of a resonator. The knowledge of complex resonant frequencies is important also for modelling spectral and/or temporal characteristics of photonic systems containing such resonators.

2. Two-dimensional model of a microresonator

Let us consider a simple 2D model of the ring and disk microresonators shown in Fig. 1. For simplicity, we will consider optical wave propagating perpendicularly to the z axis, with electric field intensity vector polarised in parallel with it. In agreement with Equation (1) the electric field intensity can be written in the form

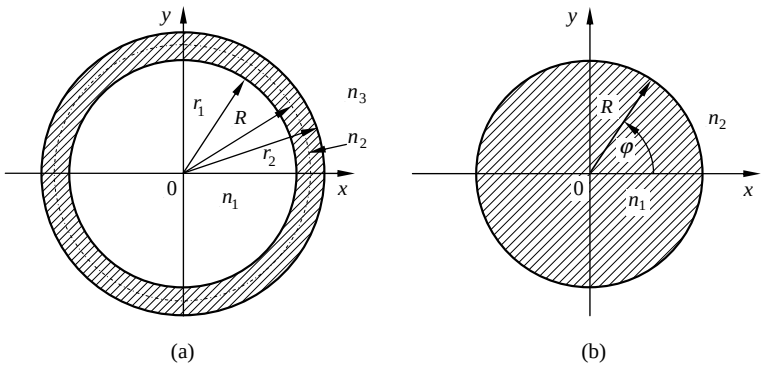

Fig. 1. A simple 2D model of a ring microresonator (a) and microdisk (b). The radius of curvature ring is chosen $R = (r_1 + r_2)/2$ for the ring and $R = r_1$ for the disk.

$$\mathbf{E}(r,\varphi) = E_z(r,\varphi)\mathbf{z}^0 = \psi(r)\exp(\mathrm{i}v\varphi)\mathbf{z}^0, \tag{7}$$

where $\psi(r)$ describes the radial dependence of the field, and v is a suitable separation constant. From Maxwell equations we find for the magnetic field intensity

$$\mathbf{H}(r,\varphi) = -\frac{\mathrm{i}}{\omega\mu}\nabla\times\mathbf{E}(r,\varphi) = \frac{1}{\omega\mu}\left(\mathrm{i}\frac{\mathrm{d}\psi}{\mathrm{d}r}\varphi^0 + \frac{v}{r}\psi\mathbf{r}^0\right)\exp(\mathrm{i}v\varphi). \tag{8}$$

The Helmholtz equation for the electric field intensity, $\Delta E_z + k_0^2 n^2(r)E_z = 0$, results in the following equation for the radial function $\psi(r)$:

$$\frac{1}{r}\frac{\mathrm{d}}{\mathrm{d}r}\left(r\frac{\mathrm{d}\psi(r)}{\mathrm{d}r}\right) + \left(k_0^2 n^2(r) - \frac{v^2}{r^2}\right)\psi(r) = 0, \tag{9}$$

where

$$n(r) = \begin{cases} n_1, & r \le r_1, \\ n_2, & r_1 < r \le r_2, \\ n_3, & r > r_2 \end{cases} \tag{10}$$

for the ring and

$$n(r) = \begin{cases} n_1, & r \le r_1 \\ n_2, & r > r_1 \end{cases} \tag{11}$$

for the disk.

The continuity of tangential field components E_z and H_φ at the interfaces $r = r_1$ and (for the ring) $r = r_2$ requires that the radial function $\psi(r)$ and its derivative $\mathrm{d}\psi/\mathrm{d}r$ are continuous at the interface(s). In the innermost radial part of the resonator, $r \le r_1$, the only physically acceptable solution of Equation 9 is apparently (Lewin *et al.* 1977)

$$\psi(r) = AJ_v(k_0 n_1 r), \tag{12}$$

where A is an arbitrary complex constant, and $J_v(z)$ is the Bessel function of the first kind of the index v and argument $k_0 n_1 r$. The other independent formal solution – Neumann function $Y_v(k_0 n_1 r)$ – has a substantial singularity at $r = 0$ and must thus be excluded.

In the outermost region, $r > r_2$ (or, for the disk, $r > r_1$), only outgoing waves radiating from the waveguide bend can propagate. For the time

dependence $\exp(-\mathrm{i}\omega t)$, the outgoing wave is described by the Hankel function of the first kind,

$$\psi(r) = DH_v^{(1)}(k_0 n_3 r). \tag{13}$$

Inside the guide of the ring, $r_1 < r \leq r_2$, both the outgoing and incoming cylindrical waves are to be considered:

$$\psi(k_0 n_2 r) = BH_v^{(1)}(k_0 n_2 r) + CH_v^{(2)}(k_0 n_2 r). \tag{14}$$

From the continuity conditions for the function $\psi(r)$ at the interfaces $r = r_1$ and $r = r_2$ of the ring resonator it follows that the amplitudes A, B, C and D are mutually bound by the system of homogeneous linear equations

$$\begin{pmatrix} n_1 J_v'(k_0 n_1 r_1) & -n_2 H_v^{(1)\prime}(k_0 n_2 r_1) & -n_2 H_v^{(2)\prime}(k_0 n_2 r_1) & 0 \\ J_v(k_0 n_1 r_1) & -H_v^{(1)}(k_0 n_2 r_1) & -H_v^{(2)}(k_0 n_2 r_1) & 0 \\ 0 & -n_2 H_v^{(1)\prime}(k_0 n_2 r_2) & -n_2 H_v^{(2)\prime}(k_0 n_2 r_2) & n_3 H_v^{(1)\prime}(k_0 n_3 r_2) \\ 0 & -H_v^{(1)}(k_0 n_2 r_2) & -H_v^{(2)}(k_0 n_2 r_2) & H_v^{(1)}(k_0 n_3 r_2) \end{pmatrix} \times \begin{pmatrix} A \\ B \\ C \\ D \end{pmatrix} = \begin{pmatrix} 0 \\ 0 \\ 0 \\ 0 \end{pmatrix}. \tag{15}$$

In the case of a disk microresonator with only one interface $r = r_1$ separating inner and outer regions, we arrive to a simpler system of two equations only,

$$\begin{pmatrix} n_1 J_v'(k_0 n_1 r_1) & n_2 H_v^{(1)\prime}(k_0 n_2 r_1) \\ J_v(k_0 n_1 r_1) & H_v^{(1)}(k_0 n_2 r_1) \end{pmatrix} \cdot \begin{pmatrix} A \\ D \end{pmatrix} = \begin{pmatrix} 0 \\ 0 \end{pmatrix}. \tag{16}$$

In these equations, the prime denotes the derivative of the corresponding cylindrical function with respect to its argument.

Let us denote the determinant of the system (15) or (16) by $\mathscr{D}(k_0, v)$. It represents the dispersion function of either a bent waveguide or a disk microresonator, the zeros of which correspond to eigenmodes of the relevant structure. For the bent waveguide, the wavelength and thus k_0 are real constants, and the corresponding dispersion equation $\mathscr{D}(k_0, v) = 0$ has to be solved for the (complex) azimuthal index v. For the microresonator, the azimuthal index v must be chosen as a suitable natural number, m, and

$\mathscr{D}(k_0, m) = 0$ becomes now the dispersion equation for the complex wavenumber k_0.

Let us note that for the transition region, $r \approx R$, where both the argument and index of the Bessel functions are comparable in magnitude, most codes for evaluation cylindrical functions of complex order and real argument fail (Pascher 2001). We have thus written our own routines using uniform asymptotic expansions (Abramovitz *et al.* 1964) that treat the behaviour of Bessel functions and their derivatives in the transition region well.

In the next section, these equations are numerically solved and the results compared and briefly discussed.

3. Numerical results

As an example, we have analysed 2D ring microresonators with the refractive indices $n_1 = n_3 = 1.6$ and $n_2 = 1.7$. The width of the waveguiding layer of the ring, $w = r_2 - r_1$, was chosen to be 1 μm, and the radius of curvature R was varied from 200 to 5 μm. In Table 1 the results of calculation using both methods are presented. For the disk microresonator with refractive indices $n_1 = 1.7$ and $n_2 = 1.6$ we present only results of the complex frequency approach.

The results in Table 1 are presented in terms of technically important parameters – the real part of the azimuthal number ν', the wavelength at resonance λ_{res}, and the resonator finesse F. To keep the calculations simple, for the bent waveguide calculations we have left the wavelength fixed at 1.3 μm. The real parts of the azimuthal indices, $\nu' = \text{Re}\{\nu\}$, in Table 1 are thus not integers. Another iteration loop in the computer code would have to

Table 1.

Radius R [μm]	Ring microresonator					Disk microresonator, complex frequency approach		
	Bent waveguide approach (λ = 1.3 μm)		Complex frequency approach					
	F	Re $\{\nu\}$	λ_{res} [μm]	F	ν	λ_{res} [μm]	F	ν
200	1.02×10^7	1605.106	1.30008	1.04×10^7	1605	1.30024	2.66×10^9	1612
100	520.67	802.779	1.29965	535.96	803	1.30082	1.64×10^5	811
80	81.22	642.368	1.30074	82.50	642	1.30094	4643.796	648
60	14.10	482.022	1.30006	14.41	482	1.30184	162.94	485
50	6.25	401.891	1.29965	6.40	402	1.30147	35.13	404
40	2.93	321.795	1.29919	3.00	322	1.30158	8.69	323
30	1.45	241.735	1.29859	1.49	242	1.29765	2.63	243
20	0.76	161.706	1.29763	0.78	162	1.29984	0.96	162
10	0.41	81.716	1.29513	0.42	82	1.29547	0.44	82
5	0.31	41.808	1.29192	0.32	42	1.29190	0.32	42

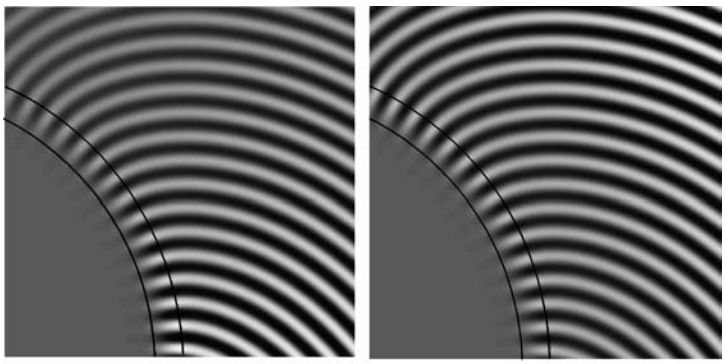

Fig. 2. Electric field distribution in the ring microresonator with $R = 10\,\mu m$ calculated using the bent guide approach (a) and the complex frequency approach (b). The guiding layer is located between the two black circle lines. The wave propagates in a counterclockwise direction.

be used that would turn v to a natural number by changing the frequency. Even without this, it is apparent that both approaches deliver essentially equivalent results, at least from the point of view of design applications – the differences in calculated finesses are technically unimportant for all values of radii of curvature.

The electric field distributions in the 2D ring resonator with the radius of curvature of 10 μm calculated with both approaches are depicted in Fig. 2. We have chosen very small radius of curvature with strong radiation losses in order to visualise the field decay along the direction of propagation in the bent guide (from bottom to top left in Fig. 2(a)). No such decay can be found in Fig. 2(b) that was obtained with the complex frequency approach.

Although both approaches give similar results, only the complex frequency approach allows one to display the field distribution in the whole microresonator in a selfconsistent way. As an example, the field distribution in the microdisk with the radius of 10 μm is plotted in Fig. 3. The wave fronts are strongly bent 'back' with respect to the counterclockwise direction of propagation, demonstrating the very strong in-plane radiation from the resonator.

Results presented in Table 1 reveal another interesting property of microresonators: the finesse of the microdisk is significantly greater than that of the microring with the same radius of curvature and the same refractive index contrast (except for very small radii that are too lossy for practical applications). The physical reason for this difference is that the field in the microdisk is more confined in the disk due to greater refractive index n_1 inside the disk; the argument $k_0 n_1 r$ of the Bessel function (12) for all $r < r_1$ is namely greater for the disk than for the ring. The radial field distributions of a ring and disk resonators with radii close to 50 μm are plotted in Fig. 4. Note that except the stronger confinement of the field inside the disk, its radiation

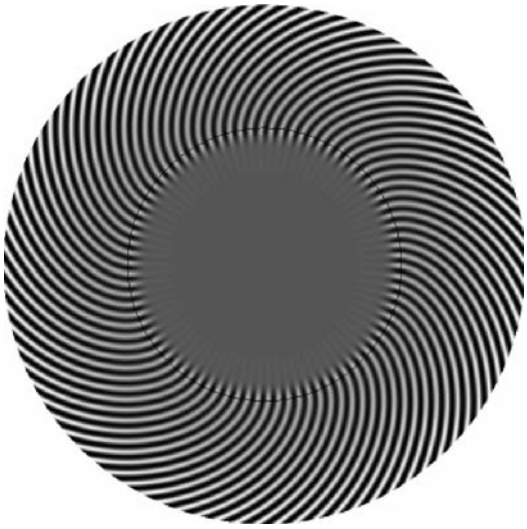

Fig. 3. Electric field distribution in the disk microresonator with $R = 10\,\mu m$ calculated using the complex frequency approach. The wave propagates counterclockwise.

field outside the resonator is weaker. It is evident that close to the centre, the fields of both resonators are very weak, as follows from Equation (12) for $k_0 n_1 r \ll \nu'$.

To estimate the field behaviour for large radii, the asymptotic expansion of the Hankel function of an integer order (Abramovitz *et al.* 1964) can be used:

$$H_\nu^{(1)}(z) \approx \sqrt{\frac{2}{\pi z}} \exp[\mathrm{i}(z - \pi\nu/2 - \pi/4)], \quad -\pi < \arg z < 2\pi. \tag{17}$$

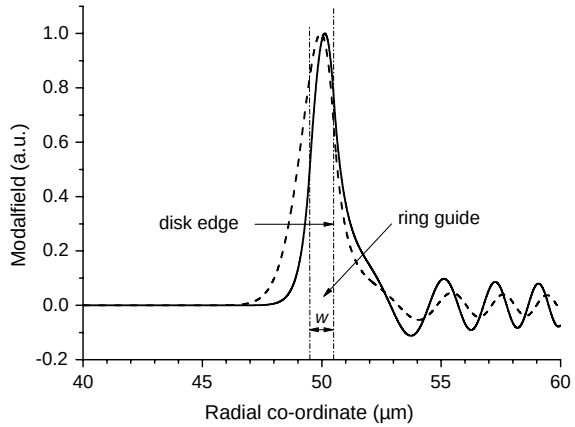

Fig. 4. Radial field distributions in the ring and disk resonators with $r_1 = 49.5\,\mu m$, $r_2 = 50.5\,\mu m$ at resonance. Solid line – ring, dashed line – disk.

According to this formula, the far-field of the resonators can be approximated by

$$E_z(r,\varphi) \approx D\sqrt{\frac{2}{\mathrm{i}\pi k_0 n_3 r}}\exp(\mathrm{i}k_0 n_3 r)\exp[iv(\varphi-\pi/2)]. \tag{18}$$

In the complex frequency approach, k_0 is complex, $k_0 = k_0' + \mathrm{i}k_0''$, with negative imaginary part, $k_0'' < 0$. The field thus *grows* for $r \to \infty$ as $(1/\sqrt{r})\exp(|k_0''|n_3 r)$. This growth can be physically explained as follows: while we observe the spatial field distribution at a particular time moment, the field at a more distant point was radiated from the resonator at an earlier time when the field was stronger.

4. Discussion and summary

Two approaches for modelling mode field distribution in ring and disk microresonators have been described. We have shown that besides the traditional approach based on the complex mode solver for bent waveguides, an alternative approach of a complex eigenfrequency can be used, too. Both methods were applied to calculate the resonance frequency and finesse of the 2D microring resonators, with essentially identical results. The complex frequency approach allows finding the field distribution in the resonator as a whole. The calculations also showed that the finesse of a disk microresonator tends to be substantially higher than that of a ring microresonator with the same radius of curvature and refractive index contrast, due to stronger radial confinement of the field in the microdisk. Differences in the spatial field distributions given by the two approaches were briefly discussed and explained using simple physical arguments.

The complex frequency approach can be applied to 3D modelling of microresonators, too. When using the coupled mode approach, the numerical difficulties are the same as those encountered in the mode-matching-based mode solver for bent guides which can be developed along the same guidelines as for straight channels (Sudbø 1993, 1994). Our paper describing the treatment of 3D resonators using the mode matching approach will be soon sent for publication elsewhere. Note that the complex frequency approach leaves the (complex) orthogonality of eigenmodes unaffected, and mode expansion problem is similar to that of the complex coordinate stretching encountered when using perfectly matched layers (Chew *et al.* 1997). Some additional numerical effort is to be exhibited, however, since for each iteration of the complex frequency, all individual eigenmodes of vertical 'slices' have to be newly computed.

Acknowledgements

This work was done in the framework of the EU project IST-2000-28018 – Next-generation Active Integrated-optic Subsystems 'NAIS'.

References

Abramovitz, M. and I.A. Stegun. *Handbook of mathematical functions*. National Bureau of Standards, Boulder, 1964.
Chew, W.C., J.M. Jin and E. Michielsen. *Microwave Opt. Technol. Lett*. **15** 383, 1997.
Chin, M.K. and S.T. Ho. *J. Lightwave Technol*. **16** 1433, 1998.
Chu, S.T., W. Pan, S. Suzuki, B.E. Little, S. Sato and Y. Kokubun. *IEEE Phot. Technol. Lett*. **11** 1138, 1999.
Klunder, D.J.W., M.L.M. Balistreri, F.C. Blom, H.J.W.M. Hoekstra, A. Driessen, L. Kuipers and N.F.v. Hulst. *J. Lightwave Technol*. **20** 519, 2002.
Lewin, L., D.C. Chang and E.F. Kuester. *Electromagnetic waves and curved structures*. Peter Peregrinus Ltd., Stevenage 1977.
Little, B.E., S.T. Chu, H.A. Haus, J. Foresi and J.-P. Laine. *J. Lightwave Technol*. **15** 998, 1977.
Little, B.E. and S.T. Chu. *IEEE Phot. Technol. Lett*. **12** 401, 2000.
Little, B.E., J.S. Foresi, G. Steinmeyer, E.R. Thoen, S.T. Chu, H.A. Haus, E.P. Ippen, L.C. Kimerling and W. Greene. *IEEE Phot. Technol. Lett*. **10** 549, 1988.
Loaiza, J.A., D.J.W. Klunder, H.F. Bulthuis, M. Lohmeyer, H.J.W.M. Hoekstra and A. Driessen. *LEOS Benelux 2000*, Delft, The Netherlands, 215, 2000.
Manolatou, C., M.J. Khan, S. Fan, P.R. Villeneuve, H.A. Haus and J.D. Joannopoulos. *IEEE J. Quantum Electron*. **35** 1322, 1999.
Pascher, W. *Opt. Quantum Electron*. **33** 433, 2001.
Sudbø, A.S. *Pure Appl. Opt*. **2** 211, 1993.
Sudbø, A.S. *Pure Appl. Opt*. **3** 381, 1994.
Yariv, A. *Electron. Lett*. **36** 321, 2000.